Infinite-Order Excitonic Bloch Equations for Asymmetric Nanostructures

M. Hawton[1] and M. M. Dignam[2]
[1]Department of Physics, Lakehead University, Thunder Bay, Ontario, Canada P7B 5E1
[2]Department of Physics, Queen's University, Kingston, Ontario, Canada K7L 3N6
(Received 27 June 2003; published 29 December 2003)

We present a new exciton-based formalism for calculating the coherent response of asymmetric semiconductor multiple quantum well structures to ultrashort optical pulses valid to infinite order in the optical field and including the self-generated intraband fields. We use these equations to calculate and explain the oscillations with time delay of peaks in the spectrally resolved degenerate four-wave mixing signals from biased semiconductor superlattices, obtaining good agreement with experiment.

DOI: 10.1103/PhysRevLett.91.267402 PACS numbers: 78.47.+p, 42.65.Re, 78.67.–n

Over the last decade, there has been a great deal of interest in the nonlinear optical response of semiconductor nanostructures to ultrashort optical pulses. Many phenomena have been treated using the dynamics controlled truncation (DCT) theory of Axt and Stahl [1], whereby the response is expanded in powers of the exciting laser field [1–3]. This theory has been very successful and correctly treats intraexcitonic and interexcitonic correlations to arbitrary order in the optical field. However, it is intrinsically a perturbative technique, while the theoretical description of many interesting nonlinear processes requires a nonperturbative approach.

The semiconductor Bloch equations (SBE's) in the Hartree-Fock (HF) approximation provide a compact description of dynamics to infinite order in the optical field [4]. They have been used to describe Rabi splitting [5] and the ac Stark effect [6]. It has been shown [7,8], however, that the HF factorization of four-particle correlation functions into products of two-particle correlation functions underestimates intraexcitonic electron-hole correlations and incorrectly predicts a rapid temporal decay of excitonic features in the intraband response.

In recent years, there has been a great deal of work on the nonlinear optical properties of asymmetric coupled quantum well systems such as biased semiconductor superlattices (BSSL's) [3,7–13]. Of particular interest has been the interplay of the interband and intraband response in two-beam degenerate four-wave mixing (FWM) experiments, where ultrashort optical pulses with wave vectors $\mathbf{k}_1$ and $\mathbf{k}_2$ separated by a delay time τ_{21} impinge on a sample [3,7–10]. The interband polarization is responsible for pump-probe, four-wave mixing, and higher-order signals, while the intraband polarization describes the coherent motion of the electrons *within* each band. In a BSSL, the electron energy levels form the so-called Wannier-Stark ladder (WSL): $E_n = E_0 + n\hbar\omega_B$, where $\omega_B \equiv eE_{\rm dc}d/\hbar$ is the Bloch frequency, d is the superlattice period, and $E_{\rm dc}$ is the applied along-axis dc electric field. Excitation of a coherent superposition of WSL states results in oscillations in the intraband polarization at ω_B. This signature of Bloch oscillations (BO's) has been seen, not only in the THz radiation generated by the intraband polarization, but also in the time-resolved and time-integrated degenerate four-wave mixing signals (TRFWM and TIFWM, respectively). These features can all be qualitatively understood using perturbative approaches such as DCT [3,7].

Recently, BO's have been observed in *spectrally resolved* four-wave mixing (SRFWM) experiments [9,10], where the peak energies of excitonic resonances were found to oscillate with the time delay, τ_{21}, at the Bloch frequency. Although it has been suggested that these oscillations result from the influence of the excitonic intraband dipole on the excitonic energies [9,10,13], the precise mechanism has never been clear and there has been some controversy regarding this interpretation [11]. It is known that third-order DCT-type calculations do not yield significant peak oscillations [3]. In fact, as we show, peak oscillations similar to the experimentally observed ones will arise only from a formalism that is infinite order in the optical field.

In this Letter, we present a new nonlinear response formalism, valid to infinite order in the optical field, that combines the essential features of both the SBE's and DCT theory for asymmetric systems. Our approach relies on the fact that, in such systems, exciton-exciton interactions are dominated by a dipole-dipole interaction and that phase space filling (PSF) effects can be relatively small at carrier densities for which exciton-exciton interactions are significant [14]. In what follows, we present our theory and calculate the TIFWM and SRFWM signals for a BSSL. We obtain oscillations in the SRFWM peak energies that are in good agreement with experimental results [9,10].

We formulate our theory on the basis of the *excitonic states* of the BSSL *in the presence of the applied dc field*, $E_{\rm dc}$. While recent work shows that treatment of PSF in an exciton basis is difficult and subtle [3,15], these problems do not arise for the densities considered here [14]. The excitons are characterized by the quantum numbers (μ, n), where μ describes the internal motion and $\mathbf{K}_n$ is the center of mass wave vector. This wave vector

 © 2003 The American Physical Society

determines the direction of the optical radiation emitted by the exciton. In degenerate FWM experiments, incident optical pulses create excitons with wave vectors $\mathbf{K}_1 \equiv \mathbf{k}_1$ and $\mathbf{K}_{-1} \equiv \mathbf{k}_2$. These excitons produce an *intraband* polarization grating with wave vectors $\mathbf{K}_{\pm 2} = \pm(\mathbf{k}_1 - \mathbf{k}_2)$ that scatter the optically created excitons into wave vectors $\mathbf{K}_3 \equiv 2\mathbf{k}_1 - \mathbf{k}_2$ and $\mathbf{K}_{-3} \equiv 2\mathbf{k}_2 - \mathbf{k}_1$. Considering all scattered excitons, the intraband grating is described by wave vectors $\mathbf{K}_m = \frac{m}{2}(\mathbf{k}_1 - \mathbf{k}_2)$ (m even) and excitons are scattered into all wave vectors $\mathbf{K}_n = \frac{1}{2}[(n+1)\mathbf{k}_1 - (n-1)\mathbf{k}_2]$ (n odd) [3]. Henceforth, we refer to signals in the FWM direction, $\mathbf{K}_{-3}$, as FWM signals, although they are to infinite order in the optical field.

Thus, for our BSSL, the Hamiltonian is given by [3]

$$H = \sum_{\mu;\, n=-n_0}^{n_0 \text{ by } 2} \hbar\omega_\mu B^\dagger_{\mu,n} B_{\mu,n} - V \sum_{n=\pm 1} (\mathbf{E}^{\text{opt}*}_n \cdot \mathbf{P}^{\text{inter}}_n + \text{H.c.}) + V \sum_{m=-2n_0}^{2n_0 \text{ by } 2} \left[\frac{1}{2\epsilon} \mathbf{P}^{\text{intra}}_{-m} - \mathbf{E}^{\text{THz}}_{\text{ext}} \delta_{m,0} \right] \cdot \mathbf{P}^{\text{intra}}_m, \quad (1)$$

where V is the system volume, ϵ is the permittivity of the BSSL, $\hbar\omega_\mu$ is the energy, and $B^\dagger_{\mu,n}$ is the creation operator of the exciton (in the dc field) in the state (μ, n) (for n odd). The fields of the incident optical pulses are given by $\text{Re}[\mathbf{E}^{\text{opt}}_n(t)] = \text{Re}[\varepsilon^{\text{opt}}_n(t) e^{-i\omega_c t}]$, where ω_c is the laser central frequency, $\varepsilon^{\text{opt}}_n(t)$ is the complex temporal envelope, and $\mathbf{E}^{\text{THz}}_{\text{ext}}(t)$ is an external THz field. The interband polarization with wave vector $\mathbf{K}_n$ (n odd) is $\mathbf{P}^{\text{inter}}_n = \frac{1}{V}\sum_\mu (\mathbf{M}_\mu B^\dagger_{\mu,-\mathbf{K}_n} + \mathbf{M}^*_\mu B_{\mu,\mathbf{K}_n})$, where $\mathbf{M}_\mu$ is the excitonic interband dipole matrix element. Finally, the intraband polarization with wave vector $\mathbf{K}_m$ ($m > 0$ and even) is $\mathbf{P}^{\text{intra}}_m = \frac{1}{V}\sum_{\mu,\mu'}\sum_n \mathbf{G}_{\mu,\mu'} B^\dagger_{\mu,n} B_{\mu',m+n}$, where $\mathbf{G}$ is the intraband dipole matrix element between two excitonic states [3], $\mathbf{P}^{\text{intra}}_{-m} = \mathbf{P}^{\text{intra}\dagger}_m$, and the sum over n is from $-n_o$ to $n_0 - m$ by 2, and n_o is an odd, positive integer [3]. The index, n_o, serves as a truncation point for the sum; if n_o is infinite, then the expression is exact. In actual calculations we increase n_o until convergence is obtained.

We use the Heisenberg equations to determine operator dynamics and truncate the hierarchy of equations by factoring the three-exciton (six-particle) correlation functions into one- and two-exciton correlation functions. This factorization is very different than that used in the SBE's, as it retains the intraexcitonic electron-hole correlations and the long range exciton-exciton correlations. It has been shown to be very accurate for the calculation of degenerate FWM signals to third order in BSSL's [3]. We account for dephasing and decoherence phenomenologically via the interband and intraband dephasing times, T_μ and $T_{\mu\nu}$, respectively. The dynamical equations for $\langle B^\dagger_{\mu,n}\rangle$ and $\langle B^\dagger_{\mu,n} B_{\nu,j}\rangle$ thus become

$$i\hbar \frac{d\langle B^\dagger_{\mu,n}\rangle}{dt} = -\hbar\left(\omega_\mu + \frac{i}{T_\mu}\right)\langle B^\dagger_{\mu,n}\rangle + \mathbf{E}^{\text{opt}*}_n \cdot \mathbf{M}^*_\mu + \sum_{\nu;\,k=-n_0}^{n_0 \text{ by } 2} \mathbf{E}^{\text{intra}*}_{n-k} \cdot \mathbf{G}_{\nu,\mu}\langle B^\dagger_{\nu,k}\rangle, \quad (2)$$

$$i\hbar \frac{d\langle B^\dagger_{\mu,n} B_{\nu,j}\rangle}{dt} = -\hbar\left(\omega_\mu - \omega_\nu + \frac{i}{T_{\mu\nu}}\right)\langle B^\dagger_{\mu,n} B_{\nu,j}\rangle + \mathbf{E}^{\text{opt}*}_n \cdot \mathbf{M}^*_\mu \langle B_{\nu,j}\rangle - \mathbf{E}^{\text{opt}}_j \cdot \mathbf{M}_\nu \langle B^\dagger_{\mu,n}\rangle + \sum_{\mu';\,k=-n_o}^{n_0 \text{ by } 2} [\mathbf{E}^{\text{intra}*}_{n-k} \cdot \mathbf{G}_{\mu',\mu}\langle B^\dagger_{\mu',k} B_{\nu,j}\rangle - \mathbf{E}^{\text{intra}}_{j-k} \cdot \mathbf{G}^*_{\mu',\nu}\langle B^\dagger_{\mu,n} B_{\mu',k}\rangle], \quad (3)$$

where $\mathbf{E}^{\text{intra}}_{-m} \equiv -\frac{1}{\varepsilon}\langle \mathbf{P}^{\text{intra}}_m\rangle + \mathbf{E}^{\text{THz}}_{\text{ext}}\delta_{m,0}$ is the total intraband field with wave vector $\mathbf{K}_m$. These dynamical equations can also be modified to include PSF [3], although, as the effects of PSF are small in this system [14], we neglect these terms for simplicity.

Note that in the above equations, the $\mathbf{K} = 0$ *internal* intraband field interacts with the excitons in exactly the same way as an *external* THz field. The dc component of this field renormalizes the excitonic energy, $\hbar\omega_\mu$, while its THz component dynamically couples levels with different μ [13]. As discussed below, it is largely the $\mathbf{K} = 0$ internal field that yields the peak oscillations in the SRFWM signal. A DCT calculation to any order will not yield these oscillations because the equation for $\langle B^\dagger_{\mu,-3}\rangle^{(n)}$ ($\langle B^\dagger_{\mu,-3}\rangle$ to order n) does not contain a term proportional to $\mathbf{E}^{\text{intra}}_0 \langle B^\dagger_{\mu,-3}\rangle^{(n)}$.

We now present calculated results for the $GaAs/Ga_{0.7}Al_{0.3}As$ superlattice used in recent experiments [9,10]: the well widths and barrier widths are 67 Å and 17 Å, respectively, the dc electric field is 15 kV/cm, and there is no *external* THz field. The single-particle BO period of this system is $\tau_B = 328$ fs, with a corresponding WSL energy spacing of $\hbar\omega_B = 12.6$ meV. The system is excited by two Gaussian optical pulses with temporal FWHM of 90 fs. The dephasing times are taken to be $T_{\text{inter}} = T_\mu = 1.0$ ps and $T_{\text{intra}} = T_{\mu\nu} = 1.5$ ps (similar to those observed in Ref. [8]), while the excitonic population decay time, $T_{\mu\mu}$, is taken to be infinite [16]. As in the experiments [9,10], the exciton areal density ranges from 10^9 to 10^{10} cm^{-2}. Only $1s$ heavy-hole excitons are included, so that the single internal quantum number μ describes an exciton in which the average along-axis electron-hole separation is approximately μd [3]. Thus, for the exciton, μ plays the role that n does for the single-particle WSL states except that the excitonic WSL is not equally spaced [3]. These states are calculated using the method described in

Ref. [12]. The neglect of excited in-plane excitonic states has been shown to be justified for central laser frequencies below the $\mu = 0$ WSL frequency [12].

Figure 1 shows the TIFWM intensity as a function of delay time. The oscillations are due to BO's of the excitonic wave packets [3,13]. The frequency of the oscillations is not precisely given by ω_B for two reasons. First, the dc component of the $\mathbf{K} = 0$ internal THz field renormalizes the excitonic energies by giving an effective dc field of $\mathbf{E}_{\rm dc} + \mathbf{E}_0^{\rm intra,dc}$; because $\mathbf{E}_0^{\rm intra,dc}$ is antiparallel to $\mathbf{E}_{\rm dc}$ for $\omega_c < \omega_0$, the BO frequency is reduced, as observed. Second, excitonic effects alter the BO frequency by changing the WSL energy spacings as mentioned above.

The large degree of nonlinearity in this system is seen in the TIFWM results obtained using different truncation indices, n_o (dotted lines in Fig. 1). For $n_0 = 3$, the TIFWM signal ($\mathbf{K}_{-3}$ direction) arises entirely from $\mathbf{k}_2$ excitons that scattered off the $\mathbf{k}_2 - \mathbf{k}_1$ grating. As n_o is increased, the excitons can scatter out of $\mathbf{K}_{-3}$ into wave vectors $\mathbf{K}_{\pm n}$ for any odd $n \leq n_0$ and perhaps even scatter back. Convergence is obtained only for $n_o \geq 9$ for this density, which demonstrates that scattering into wave vectors as large as $\mathbf{K}_{\pm 9}$ is clearly important and thus a third-order DCT approach is not adequate. The multiple scattering and the high degree of nonlinearity is also evidenced in the fact that the intensities in the $\mathbf{K}_{-5} = 3\mathbf{k}_2 - 2\mathbf{k}_1$ and $\mathbf{K}_{-7} = 4\mathbf{k}_2 - 3\mathbf{k}_1$ directions, also shown in Fig. 1, are comparable to the FWM intensity.

In Fig. 2 we plot the SRFWM signal for a sequence of delay times. The spectral peaks are associated with different excitonic states (as indicated in the figure). The peaks do not occur precisely at the single-exciton energies, ω_μ, due to the polarization-induced reduction of the applied dc field discussed above. More importantly, note that the peak positions depend significantly on the time delay, τ_{21}.

To see the peak oscillations more clearly, we plot in Fig. 3 the energy of the $\mu = -1$ peak relative to $\hbar\omega_{-1}$ as a function of τ_{21} for different exciton densities. As can be seen, and in agreement with experiment, the peak's energy oscillates as a function of τ_{21} with period given approximately by τ_B. The oscillations can be largely understood as arising from quantum interference between multiple paths from the ground state to the excitonic state $(\mu, -3)$. This can be seen through a simplified perturbative treament illustrated in the inset to Fig. 2. In the left-hand path, an exciton with wave vector $\mathbf{K}_{-1} = \mathbf{k}_2$ and energy $\hbar\omega_{\rm op}$ is created by the second optical pulse; it then scatters off the $\mathbf{K}_{-2}$ grating into $\mathbf{K}_{-3}$, absorbing a photon of energy $\hbar\omega_{\rm intra}^G \simeq 0, \pm\hbar\omega_B$. In the right-hand path, the exciton additionally interacts with the spatially uniform field, $E_0^{\rm intra}(t)$, absorbing a photon of energy $\hbar\omega_{\rm intra}^0 \simeq 0, \pm\hbar\omega_B$ before reaching the final state $(\mu, -3)$. To perturbatively calculate $\langle B^\dagger_{\mu,\pm1}\rangle^{(1)}$ and $\langle B^\dagger_{\mu,m}\rangle^{(2)}$ we set $\mathbf{E}^{\rm intra} = 0$ in Eqs. (2) and (3) and include the dominant contributions to obtain $\langle B^\dagger_{\mu,-1}\rangle^{(1)}$ and $E_0^{\rm intra(2)}(\omega_B) \sim e^{-i\omega_B\tau_{21}/2}\cos(\omega_B\tau_{21}/2)$, respectively. Substituting in (2) we then obtain $\langle B^\dagger_{\mu,-3}\rangle^{(3)}$ which gives the polarization due to the left-hand path as $P_{-3}^{(L)}(\omega) \sim [\omega - \omega_\mu + i/T_{\rm inter}]^{-2}$ and, using $\langle B^\dagger_{\mu,-2}\rangle^{(2)}$ and $\langle B^\dagger_{\mu,-3}\rangle^{(3)}$, we obtain $P_{-3}^{(R)}(\omega) \sim P_{-3}^{(1)}(\omega)E_0^{\rm intra}(\omega_B)/[\omega - \omega_\mu + i/T_{\rm inter}]$. It can be simply shown that interference between these two contributions yields oscillations in the SRFWM peaks that depend on the amplitude and phase of $E_0^{\rm intra}(\omega_B)$.

The oscillation of $E_0^{\rm intra}(\omega_B)$ with time delay is due to alternating constructive and destructive interference

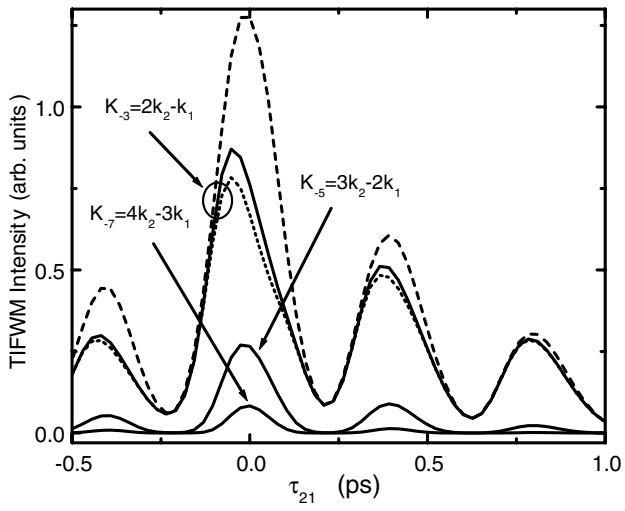

FIG. 1. The time-integrated intensity versus τ_{21} for $\omega_c = \omega_0 - 2.27\omega_B$, $n_o = 13$, and a density of 6.36×10^9 cm^{-2} for the three different directions, $\mathbf{K}_n$ indicated. For $\mathbf{K}_{-3}$, results for $n_0 = 3$ (dashed line) and 5 (dotted line) are also plotted.

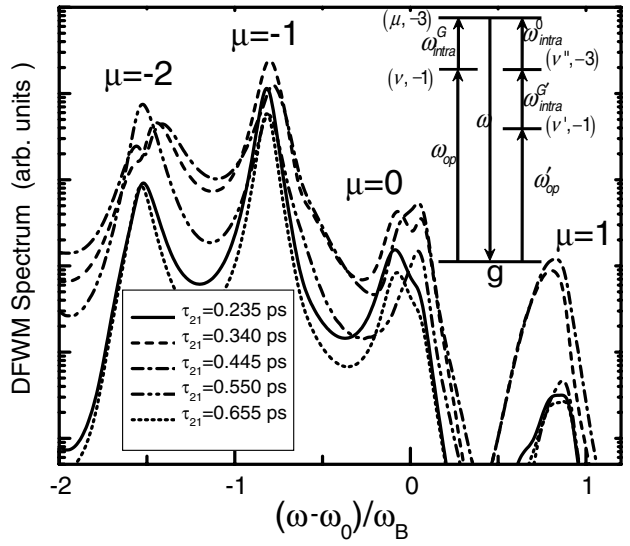

FIG. 2. SRFWM intensity versus frequency at $\omega_c = \omega_0 - 2.27\omega_B$ and a density of 9.3×10^9 cm^{-2} for a sequence of delay times. The inset is described in the text.

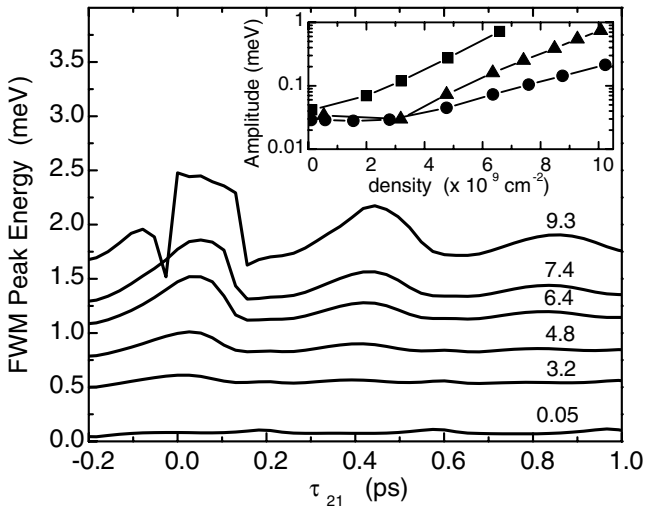

FIG. 3. The $\mu = -1$ SRFWM peak energy relative to $\hbar\omega_{-1}$ versus τ_{21} at $\omega_c = \omega_0 - 2.27\omega_B$ for the densities given above each curve (in units of 10^9 cm^{-2}). The curve offsets are a real effect due to intraband renormalization of the dc field. The inset shows peak oscillation amplitude as a function of density for $(\omega_c - \omega_0)/\omega_B = -1.24$ (circles), -2.27 (triangles), and -2.83 (squares).

between the Bloch oscillating intraband polarizations created by the first and second pulses. Thus, the periodic oscillations in the SRFWM *peak positions* arise due to the quantum interference between two-photon and three-photon processes. When the full equations are solved, one finds that higher-order nonlinearities play an important role, yielding an oscillation amplitude that depends nonlinearly on exciton density. In the inset to Fig. 3, we show the amplitude of the peak oscillations (defined to be the energy difference between the first dip after $\tau_{21} = 0$ and the peak that follows) as a function of density for three different central laser frequencies. Note that at low densities, the oscillation amplitude is independent of density. In this regime, the peak oscillations are due to small effects that occur even to third order in the optical field. At higher densities the amplitudes increase superlinearly with density due to multiple scatterings from the intraband polarization grating. At the highest density of 9.3×10^9 cm^{-2}, the sudden change in peak energy near $\tau_{21} = 0.16$ ps results from a splitting of the $\mu = -1$ peak, similar to that seen in Fig. 2 for the $\mu = 0$ peak for $\tau_{21} = 0.34$ ps.

Most of the features of the calculated peak oscillations agree with experiment: the phase, frequency, dependence on ω_c, and large amplitude at $\tau_{21} = 0$ are all in general agreement [9,10]. However, the amplitude of the peak oscillation is considerably smaller than that obtained experimentally. For example, for $\omega_c = \omega_0 - 2.27\omega_B$, and a density of 10^{10} cm^{-2}, the calculated amplitude is roughly 0.6 meV, while the experimental amplitude is approximately 2.3 meV [10]. We believe that this difference is largely due to the screening of exciton-exciton interactions via incoherent carriers. As discussed in Ref. [10], this plasma screening will considerably decrease the dielectric constant at the Bloch frequency. We find, for example, that a decrease in ϵ/ϵ_o from 12.5 to 8 can result in an increase in the peak-oscillation amplitude by a factor of 3 or more, bringing the calculated and experimental results into quite good agreement. For simplicity, in this work, we have a static permittivity of 12.5 ϵ_o but plan to use a dynamic model in future work.

In summary, we have developed a new infinite order excitonic system of equations for calculating the nonlinear optical response of asymmetric semiconductor nanostructures. We have used these equations to reproduce for the first time the experimentally observed [9,10] oscillations in the SRFWM signals from BSSL's.

We thank Karl Leo and Lijun Yang for valuable discussions. This work was supported in part by the Natural Sciences and Engineering Research Council of Canada.

[1] V. M. Axt and A. Stahl, Z. Phys. B **93**, 195 (1994).
[2] Margaret Hawton and Delene Nelson, Phys. Rev. B **57**, 4000 (1998).
[3] M. M. Dignam and M. Hawton, Phys. Rev. B **67**, 035329 (2003).
[4] H. Haug and S. W. Koch, *Quantum Theory of the Optical and Electronic Properties of Semiconductors* (World Scientific, Singapore, 1995).
[5] S. Schmitt-Rink, D. S. Chemla, and H. Haug, Phys. Rev. B **37**, 941 (1988).
[6] R. Binder, S. W. Koch, M. Lindberg, W. Schafer, and F. Jahnke, Phys. Rev. B **43**, 6520 (1991).
[7] V. M. Axt, G. Bartels, and A. Stahl, Phys. Rev. Lett. **76**, 2543 (1996).
[8] P. H. Bolivar, F. Wolter, A. Muller, H. G. Roskos, H. Kurz, and K. Köhler, Phys. Rev. Lett. **78**, 2232 (1997).
[9] V. G. Lyssenko, G. Valusis, F. Löser, T. Hasche, K. Leo, M. M. Dignam, and K. Köhler, Phys. Rev. Lett. **79**, 301 (1997).
[10] F. Löser, M. M. Dignam, Yu. A. Kosevich, K. Köhler, and K. Leo, Phys. Rev. Lett. **85**, 4763 (2000).
[11] Ren-Bao Liu and Bang-Fen Zhu, Phys. Rev. B **59**, 5759 (1999).
[12] M. Dignam, J. E. Sipe, and J. Shah, Phys. Rev. B **49**, 10 502 (1994).
[13] M. M. Dignam, Phys. Rev. B **59**, 5770 (1999).
[14] PSF effects go as n/n_0, where n is the areal density and n_0 is the inverse of the single $1s$ exciton area which equals 2×10^{11}/cm^2 for GaAs. In this work, we consider only areal exciton densities up to 10^{10}/cm^2 and so the effects of PSF are small.
[15] S. Okumura and T. Ogawa, Phys. Rev. B **65**, 035105 (2001); M. Combescot and O. Betbeder-Matibet, Europhys. Lett. **58**, 87 (2002).
[16] We find that finite population decay times have little qualitative effect on the results presented here.